Supporting information

Constructing High-Performance Supercapacitors and Electrochemical Water Splitting Electrode Material through Core-Shell Structured Co$_9$S$_8$@Ni(OH)$_2$ Nanosheets

Song-Lin Xu[a], Rong-Da Zhao[a,*] Rui-Yu Li[a], Jia Li[a], Jun Xiang, Fang-Yu Guo[b,*],

Jingang Qi[a], Liang-Liu[a], Fu-Fa Wu [a,*]

[a]School of Materials Science and Engineering, Liaoning University of Technology,

Jinzhou, 121001, P. R. China

[b]College of Science, National University of Defense Technology, Changsha, Hunan

410073, P. R. China

Correspondences should be addressed: rongdazhaoln@126.com; gfy88520@126.com;

Experiments, Characterization and Calculation

Cobalt nitrate hexahydrate, nickel nitrate hexahydrate, sodium sulfide nonahydrate, urea, ammonium fluoride, potassium hydroxide, absolute ethanol, hydrochloric acid (HCl), Pt/C , and nickel foam were used in this experiment. All chemicals were analytical grade and purchased from Sigma-Aldrich chemical company without further purification. All aqueous solutions were prepared using deionized (DI) water.

Analytical grade chemicals were selected for this experiment. The pretreatment procedure involved removing the oxide layer from the surface of foam nickel using a 0.1 M HCl solution, followed by cleansing with anhydrous ethanol and deionized water to eliminate impurities. The resulting foam nickel was then dried in air.

In 70 mL of distilled water, 2 mmol of $Co(NO_3)_2 \cdot 6H_2O$, 5 mmol of CH_4N_2O (urea), and 2 mmol of NH_4F (ammonium fluoride) were dissolved. After thorough stirring, the solution was transferred to a 100 mL hydrothermal kettle. A clean piece of foam nickel was immersed in the solution, and the kettle was sealed before being placed in an oven to react at 120°C for 6 hours.

Following the reaction, the foam nickel substrate was rinsed three times with deionized water and anhydrous ethanol to remove any residual reactants. Subsequently, it was dried at 60°C for a minimum of 12 hours, followed by annealing in air at 350°C for 2 hours.

For the sulfidation process, 0.35 g of $Na_2S \cdot 9H_2O$ was dissolved in 60 mL of deionized water and stirred for 30 minutes. The resulting solution was transferred to a

100 mL reaction container, sealed, and placed in the oven at 120°C for 4 hours. Following this step, the sample underwent another round of rinsing three times with deionized water and anhydrous ethanol before being dried at 60°C for at least 6 hours, resulting in the formation of the final electrode material.

Using a method similar to the aforementioned process, the prepared Co_9S_8 nanosheet electrode material was placed in a 100 ml hydrothermal kettle. The solution consisted of 1.5 mmol $Ni(NO_3)_2 \cdot 6H_2O$ and 3 mmol of urea. The material was maintained at 120°C for 2 hours, after which the sample was washed and dried to yield the $Co_9S_8@Ni(OH)_2$ composite material.

The crystal structure and phase composition of the samples were characterized by an X-ray diffractometer (XRD, D/max-2500/PC) with Cu-Kα radiation. The XRD measurements were conducted at an accelerating voltage of 100 kV, a tube current of 40 mA, a scanning range from 0 to 90°, and a scanning speed of 8°/min. The elemental composition and valence states were characterized by X-ray photoelectron spectroscopy (XPS, ESCALAB250). The microstructures of the samples were examined by field emission scanning electron microscopy (SEM, Zeiss-Sigma 500). Transmission electron microscopy (TEM, JEM2100F) was used to examine the microstructure of the sample.

Electrode Materials: Sample preparation was carried out for testing within a three-electrode configuration using an electrochemical workstation (CHI660E), immersed in a 3 M KOH aqueous solution. These samples, each measuring 1 cm in diameter and comprising a platinum plate and Hg/HgO electrodes, served as the

working, counter, and reference electrodes, respectively. The functionality of the SC

electrodes was assessed using cyclic voltammetry (CV) and electrochemical impedance

spectroscopy (EIS). The specific and areal capacitances were calculated from the

galvanostatic charge-discharge (GCD) curves, employing the following formula：

$$C_s = \frac{I\Delta t_d}{m} \tag{1}$$

$$C_A = \frac{I\Delta t_d}{S} \tag{2}$$

Where I and Δt_d represent the set current value and the discharge time, respectively. m

represents the mass of the active material in the electrodes, and S denotes the geometric

area of the electrode.

Assembly of asymmetric supercapacitors: The Active carbon (AC) electrodes

served as the cathode, while the $Co_9S_8@Ni(OH)_2$ nanocomposite structure served as

the anode, and the electrolyte was composed of Polyvinyl alcohol-KOH (PVA-KOH)

gel. For the preparation of the electrolyte, 2g of PVA was introduced into 20ml of

deionized water, while 2g of KOH was dissolved in 5ml of deionized water. The

mixtures were stirred at 80°C in a water bath until they became clear, signifying

complete dissolution. Subsequently, the solutions were set aside for subsequent

application. To craft the AC electrode, a slurry was prepared by mixing AC, acetylene

black, and polyvinylidene fluoride in an 8:1:1 mass ratio. The slurry was then coated

onto nickel foam and dried at 60°C for 24 hours to form the electrode.

For the synthesis of the gel electrolyte, the method involved dissolving 2g of PVA

in 15ml of deionized water, followed by stirring at 80°C for 30 minutes to ensure

complete dissolution. Then, a potassium hydroxide solution with a concentration of 0.4

g mL^{-1} was added dropwise to the PVA solution while stirring, and stirring continued until no bubbles were present, indicating thorough mixing.

Before assembly, the prepared electrode materials were immersed in the PVA-KOH gel electrolyte at room temperature for 25 minutes to allow for electrolyte infiltration and wetting of the electrode surfaces. Finally, a separator was used to separate the negative electrode from the positive electrode, and any air bubbles present in the electrode materials were removed using clean tweezers. The assembly was then sealed with an aluminum plastic film.

Durability assessments of the electrodes and supercapacitors were conducted using the Land Battery Test System (CT2001A), ensuring comprehensive evaluation of the electrochemical performance of the system over extended cycling periods.

The energy density (E, Wh / Kg) and power density (P, W / Kg) were evaluated according to the following Equations:

$$E = \frac{1}{2}CV^2 \tag{3}$$

$$P = \frac{3600E}{\Delta t} \tag{4}$$

In a 1 M KOH solution (pH = 13.7), the performance of the samples for both the Hydrogen Evolution Reaction (HER) and the Oxygen Evolution Reaction (OER) was evaluated using a three-electrode setup. Techniques including cyclic voltammetry (CV), linear sweep voltammetry (LSV), and I-t curves were utilized to assess the electrocatalytic activity, with CV scan rates ranging from 5 to 50 mV s^{-1}. For LSV, rates were set at 2 mV s^{-1} for OER and 5 mV s^{-1} for both HER and water splitting activities. These measurements were conducted on an electrochemical workstation,

equipped with automatic 90% infrared compensation. The electrodes were composed of prepared samples measuring 0.5 cm × 0.5 cm and Hg/HgO as the working and reference electrodes, respectively, with a graphite rod for HER and a Pt plate for OER as counter electrodes. Potentials were standardized to the Reversible Hydrogen Electrode (RHE) scale according to the Nernst equation, $E_{RHE} = E_{Hg/HgO} + 0.098 + 0.059 \times pH$, and OER overpotentials (η) were determined by the equation, $\eta = E_{RHE} - 1.23$.

Figure S1 presents the SEM and EDS images detailing the morphology and elemental composition of Co_9S_8 and $Co_9S_8@Ni(OH)_2$. In Figure S1a, the morphology of Co_9S_8 nanowires is observed, exhibiting a uniform and dense growth on the foam nickel substrate, forming fine grass-like structures. The homogeneous and dense growth enhances the electrode's effective surface area, thereby amplifying its electrochemical reactivity. Furthermore, the nanowire morphology facilitates increased electron transfer rates, potentially boosting the electrode's electrochemical performance. Figure S1b depicts the layered growth of $Ni(OH)_2$ nanoplates on the Co_9S_8 nanowires. This core-shell structure indicates improved electrode stability and charge transport efficiency. The $Ni(OH)_2$ nanoplates' growth provides additional active sites and exhibits good interconnectivity and open spaces between the plates, favoring rapid ion diffusion and electron transport. In Figure S1c, the EDS analysis confirms the presence of Co, S, Ni, and O in the finely structured grass-like nanowires of Co_9S_8, thus validating the material's composition. Figure S1d illustrates the scanning electron microscopy (SEM) image of $Co_9S_8@Ni(OH)_2$ after electrochemical cycling. Upon meticulous examination, it is apparent that the morphology of the material remains consistent before and after electrochemical cycling, underscoring its structural stability. Notably, the inset in Figure S1d presents an enlarged observation of the material, further validating its high structural stability during electrolysis or charge-discharge processes. This finding emphasizes the potential advantage of $Co_9S_8@Ni(OH)_2$ as an electrochemical material and provides robust support for its application in the field of electrochemical energy storage.

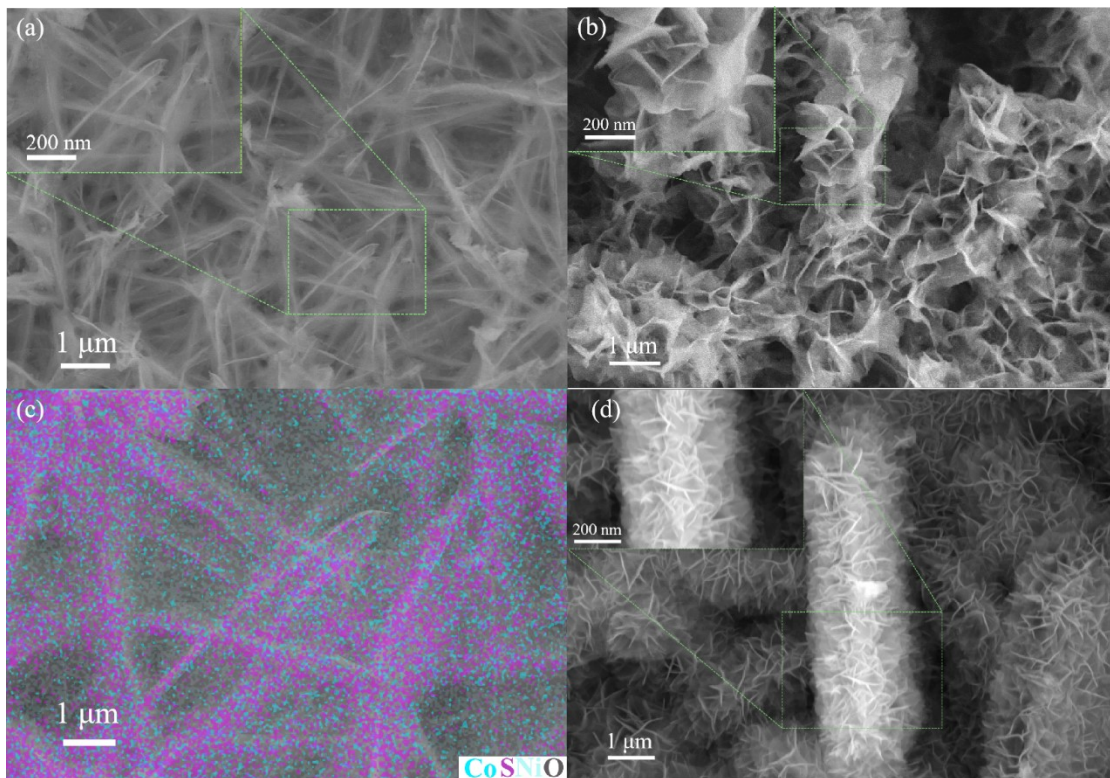**Figure S1. Songlin Xu et al.**

Figure S1. SEM and EDS images of Co_9S_8 and $Co_9S_8@Ni(OH)_2$. (a) SEM image of Co_9S_8, (b) SEM image of $Co_9S_8@Ni(OH)_2$, (c) EDS spectrum of Co_9S_8, (d) SEM image of $Co_9S_8@Ni(OH)_2$ after electrochemical cycling.

Table S1

Electrochemical performance comparison of the Core-Shell Structured $Co_9S_8@Ni(OH)_2$ Nanosheets electrode with previous literatures.

Materials	Capacity	Current density	Ref.
r-NiCo$_2$S$_4$ HSs	763.5 C g^{-1}	1 A/g	[39]
Al-doped β-NiS	697.3C g^{-1}	1 A/g	[40]
NizS$_6$	844.20 C g^{-1}	1 A/g	[41]
Co$_9$S$_8$–Ni$_3$S$_4$	861.50 C g^{-1}	1 A/g	[42]
CoMoO$_4$@NCS	510 C g^{-1}	0.5 A/g	[43]
MoSe$_2$–Ni(OH)$_2$	528.75 C g^{-1}	1 A/g	[44]
CPCN–NSs/NCS NPs	622.8 C g^{-1}	1 A/g	[45]
Co$_9$S$_8$@Ni(OH)$_2$	884.8 C g^{-1}	1 A/g	This work

Table S2

Comparison of electrochemical performances with other different materials.

Electrode materials	Energy density (Wh kg^{-1})	Power density (W Kg^{-1})	Life span/cycles	Capacitance retention (%)	Ref.
TY-NiCo-LDH/Co$_9$S$_8$//AC	38/31.1	800/8000	5000	93.1	[57]
Ni-Co LDH/Co$_9$S$_8$//AC	50/38	839/9118	5000	86.4	[58]
M-NiCo-LDH/Co$_9$S$_8$//AC	39/30.1	2400/7400	10000	90.9	[59]
C-LDH/Co$_9$S$_8$ nanocages	47.3/38.0	1505/9115	10000	80.9	[60]
MnCo$_2$O$_4$@Co$_3$O$_4$// AC	31	208.5	8000	101.2	[61]
AC/ZnS-Ni$_7$S$_6$/Ni(OH)$_2$//AC	48.99	800	3000	90.6	[62]
Co$_9$S$_8$@Ni(OH)$_2$//AC	60.76/134.26	35280/3528	15000	85.3	This work

Table S3

Electrocatalytic performance comparison of the Core-Shell Structured $Co_9S_8@Ni(OH)_2$ Nanosheets catalyst with reported catalysts.

Materials	Performances	Electrolyte	η (mV)	Ref.
NiCo-LDH/ZnCo$_2$O$_4$	OER	1 M KOH	260 (10 mA cm^{-2})	[63]
NiCo-LDH/NiCo-S sheets	OER	1 M KOH	303 (20 mA cm^{-2})	[64]
CoP@FeCoP	OER	1 M KOH	238 (10 mA cm^{-2})	[65]
Se-(NiCo)Sx/(OH)x	OER	1 M KOH	155 (10 mA cm^{-2})	[66]
NixCo$_3$-xO$_4$	HER	1 M KOH	170 (10 mA cm^{-2})	[67]
Cu@CoFe-LDH	HER	1 M KOH	171 (10 mA cm^{-2})	[68]
MOF-V-Ni$_3$S$_2$/NF	HER	1 M KOH	118.1 mV (10 mA cm^{-2})	[69]
Co$_9$S$_8$@Ni(OH)$_2$	HER	1 M KOH	92.7 mV (10 mA cm^{-2})	This work
Co$_9$S$_8$@Ni(OH)$_2$	OER	1 M KOH	169.3 mV (10 mA cm^{-2})	This work